

# Overdamped dynamics of particles with repulsive power-law interactions

André A. Moreira,<sup>1,2</sup> César M. Vieira,<sup>1,3</sup> Humberto A. Carmona,<sup>1</sup> José S. Andrade, Jr.,<sup>1,2</sup> and Constantino Tsallis<sup>4,2,5,6</sup>

<sup>1</sup>*Departamento de Física, Universidade Federal do Ceará, 60451-970 Fortaleza, Brazil*

<sup>2</sup>*National Institute of Science and Technology of Complex Systems, Rua Xavier Sigaud 150, 22290-180 Rio de Janeiro, RJ, Brazil*

<sup>3</sup>*Instituto Federal de Educação, Ciência e Tecnologia do Ceará, 62580-000 Acaraú, Brazil*

<sup>4</sup>*Centro Brasileiro de Pesquisas Físicas, Rua Xavier Sigaud 150, 22290-180 Rio de Janeiro, RJ, Brazil*

<sup>5</sup>*Santa Fe Institute, 1399 Hyde Park Road, New Mexico 87501, USA*

<sup>6</sup>*Complexity Science Hub Vienna, Josefstadter Strasse 39, 1080 Vienna, Austria*

We investigate the dynamics of overdamped  $D$ -dimensional systems of particles repulsively interacting through short-ranged power-law potentials,  $V(r) \sim r^{-\lambda}$  ( $\lambda/D > 1$ ). We show that such systems obey a non-linear diffusion equation, and that their stationary state extremizes a  $q$ -generalized nonadditive entropy. Here we focus on the dynamical evolution of these systems. Our first-principle  $D = 1, 2$  many-body numerical simulations (based on Newton's law) confirm the predictions obtained from the time-dependent solution of the non-linear diffusion equation, and show that the one-particle space-distribution  $P(x, t)$  appears to follow a compact-support  $q$ -Gaussian form, with  $q = 1 - \lambda/D$ . We also calculate the velocity distributions  $P(v_x, t)$  and, interestingly enough, they follow the same  $q$ -Gaussian form (apparently precisely for  $D = 1$ , and nearly so for  $D = 2$ ). The satisfactory match between the continuum description and the molecular dynamics simulations in a more general, time-dependent, framework neatly confirms the idea that the present dissipative systems indeed represent suitable applications of the  $q$ -generalized thermostistical theory.

## I. INTRODUCTION

Dissipative systems of repulsive particles are representative of many physical phenomena in nature, including for instance, type-II superconductors [1–7], complex plasmas [8, 9], and colloidal systems [10–12]. In the overdamped limit, the equations of motion for such systems take the form of a first order differential equation, where the velocity of the particles is proportional to the force over them,  $\mathbf{v}_i = \mathbf{F}_i/\gamma$ . A recent work [13] has shown that for a wide variety of possible repulsive potentials the local density  $\rho(\mathbf{r}, t)$  of these overdamped repulsive particles should follow a nonlinear diffusion equation in the form

$$\gamma \frac{\partial \rho}{\partial t} = \nabla \cdot \{ \rho [ \nabla U_{ext} + a(\rho) \nabla \rho ] \}, \quad (1)$$

where  $U_{ext}(\mathbf{r})$  is an applied external potential.

The function  $a(\rho)$  can be obtained from the potential energy  $U_1$  of a particle in the homogeneous state of density  $\rho$  [13],

$$a(\rho) = 2 \frac{dU_1}{d\rho} + \rho \frac{d^2 U_1}{d\rho^2}. \quad (2)$$

Determining  $U_1$  depends on the knowledge of the interaction potential and on the microscopic structure in which the particles rest in the homogeneous state [13]. As mentioned, the applicability of this approach is restricted to systems of overdamped particles interacting through a short-ranged repulsive potential. More precisely, for large distances  $r$ , the interaction potential  $V(r)$  should decay faster than  $r^{-D}$ , where  $D$  is the dimensionality of the system. The form of  $a(\rho)$  is also influenced by the way the potential diverges at the origin. If the potential diverges

at the origin slower than  $r^{-D}$ ,  $a(\rho)$  should converge to a finite value for densities  $\rho$  that are sufficiently large. Conversely, for potentials that diverge faster than  $r^{-D}$  at the origin, the energy per particle  $U_1$  grows faster than linearly with the density  $\rho$ , and  $a(\rho)$  never converges to a fixed value, regardless of the density  $\rho$  [13]. In the case where the interaction potential is a power law,  $V_{ij} = \epsilon(r_{ij}/\sigma)^{-\lambda}$ , with  $\lambda > D$ ,  $\sigma > 0$  and  $\epsilon > 0$ , Eq. (1) can be written as

$$\gamma \frac{\partial \rho}{\partial t} = \nabla \cdot \left[ \rho \left( \nabla U_{ext} + C_\lambda \rho^{\frac{\lambda}{D}-1} \nabla \rho \right) \right], \quad (3)$$

where the constant  $C_\lambda$  can be computed from the structure of the homogeneous state [13]. More recently, for this family of repulsive potentials, a consistent thermodynamic framework was developed, and thermodynamic potentials, Maxwell relations, and response functions could be obtained [14].

Here, we analytically obtain time-dependent solutions for Eq. (3),  $\rho(x, t)$ , for the case of a parabolic confining potential,  $U_{ext} = -kx^2/2$  ( $k > 0$ ), showing that they possess the form of  $q$ -Gaussian distributions [15–18], as well as the dynamics of type-II superconducting vortices [19, 20]. We compare these solutions with the results obtained from computer simulations, where the equations of motion are solved numerically, and find a good agreement. Moreover, our results show that, for the class of solutions we obtain, the velocities of the particles should be proportional to their position, that is,  $v_i \sim x_i$ , as also observed in Ref. [19] for the London potential. This suggests that the velocity distribution should follow closely the same expected form for the density profile, namely, a  $q$ -Gaussian. As we show, however, due to the readjustment of the local spatial structure of

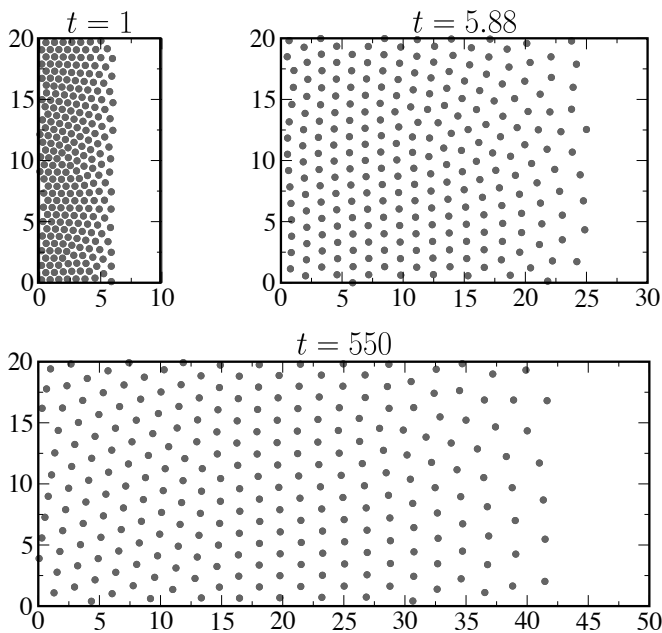


FIG. 1. Snapshots of the configuration of the system in three different moments of the dynamics. Due to the symmetry we show only the  $x > 0$  half of the system. The particles start in a very narrow region and invade the system as time goes, eventually reaching an equilibrium position. This system comprises  $N = 500$  particles, interacting through a potential  $V_{ij} = \epsilon(r_{ij}/\sigma)^{-\lambda}$ , with  $\lambda = 4$ , in a cell of lateral length  $L_y = 20\sigma$ , and confined by an external force  $-kx$  with  $k = 1 \times 10^{-6}\epsilon/\sigma^2$ .

the system as the surrounding density changes, it generates, for  $D > 1$ , an extra noise that leads, as compared to  $q$ -Gaussians, to small deviations in the shape of the velocity distributions at the highest velocities.

## II. MODEL SOLUTION

In the present work, the systems that we model consist of  $N$  particles interacting through the above mentioned potential  $V_{ij} = \epsilon(r_{ij}/\sigma)^{-\lambda}$  and confined in the  $x$ -direction by the external potential  $U_{ext}$ . For the case of two dimensions, in the  $y$ -direction the simulation cell has a finite length  $L_y$  and periodic boundary conditions are imposed. See Fig. 1 for a view of a 2D system in different moments of the dynamics. In this case, it is reasonable to expect the density to be independent on  $y$ , so that Eq. (3) can be written as

$$\gamma \frac{\partial \rho}{\partial t} = \frac{\partial}{\partial x} \left[ \rho \left( kx + C_\lambda \rho^{\frac{\lambda}{D}-1} \frac{\partial \rho}{\partial x} \right) \right]. \quad (4)$$

One may find solutions of Eq. (4) by making use of the similarity hypothesis [21],

$$\rho(x, t) = \frac{g(z)}{f(t)}, \quad (5)$$

with  $z = x/f(t)$ . Using this in Eq. (4), we obtain

$$\frac{f^{1+\frac{\lambda}{D}}}{C_\lambda} \left( \frac{df}{dt} + kf \right) = - \frac{\frac{d}{dz} \left( g^{\frac{\lambda}{D}} \frac{dg}{dz} \right)}{\frac{d}{dz} (gz)}. \quad (6)$$

The left side of Eq. (6) depends on  $t$ , while the right side depends on  $z$ . The only possible solution is that both sides are equal to some constant,  $\nu$ . From that, the left side becomes

$$\frac{df}{dt} = \frac{\nu C_\lambda}{f^{\frac{\lambda}{D}+1}} - kf \quad (7)$$

while the right side can be written as

$$\frac{d}{dz} \left( g^{\frac{\lambda}{D}} \frac{dg}{dz} + \nu gz \right) = 0. \quad (8)$$

To solve Eq. (8) we consider the boundary condition  $g(1) = 0$ , leading to

$$g = \left[ \frac{\lambda \nu}{2D} (1 - z^2) \right]^{\frac{D}{\lambda}}, \quad (9)$$

that is, the shape of the density profile is a  $q$ -Gaussian with  $q = 1 - \lambda/D$  at any instant of time. The normalization condition,  $\int \rho(x, t) dx = n$ , leads to  $\int g dz = n$ , where  $n = N$  for  $D = 1$  and  $n = N/L_y$  for  $D = 2$ , remembering that  $L_y$  gives the thickness of the simulation cell and  $N$  the number of particles. This allows us to determine the value of  $\nu$ , namely

$$\nu = \frac{2D}{\lambda} \left[ n \frac{\Gamma(\frac{3}{2} + \frac{D}{\lambda})}{\Gamma(1 + \frac{D}{\lambda}) \sqrt{\pi}} \right]^{\frac{\lambda}{D}}. \quad (10)$$

It is also visible from this solution that  $f(t)$  is the point where  $\rho(f(t), t) = 0$ , that is,  $f(t)$  is the edge of the distribution. Solving Eq. (7) we obtain

$$f(t) = \left\{ \frac{\nu C_\lambda}{k} \left[ 1 - e^{-k(\frac{\lambda}{D}+2)(t-t_0)} \right] \right\}^{\frac{D}{\lambda+2D}}, \quad (11)$$

where  $t_0$  is a free parameter that depends on the initial condition. Since in our numerical simulations we start with all particles confined in a narrow stripe,  $t_0 = 0$  should fit well our numerical results. In Fig. 2 we show the curves of  $f(t)$  and  $\dot{f}(t) \equiv df/dt$  for each instant of time  $t$  considering  $\lambda = 2$  and  $\lambda = 3$  in one dimension, and  $\lambda = 4$  and  $\lambda = 6$  in two dimensions. These curves were obtained from Eq. (11). As we show in what follows, these predictions closely agree with the results from the numerical simulations.

## III. NUMERICAL SIMULATIONS

Figure 3 shows the density profile at different moments of the dynamics for one dimensional systems. To obtain

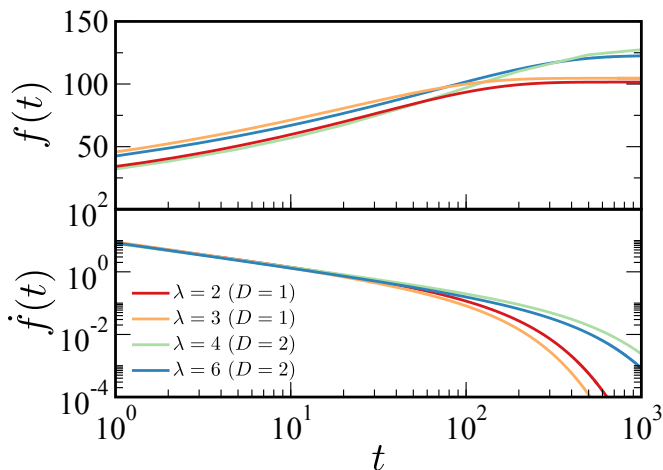


FIG. 2. Curves of  $f(t)$  for  $D = 1$  ( $\lambda = 2$  and  $3$ ) and  $D = 2$  ( $\lambda = 4$  and  $6$ ) obtained from Eq. (11) and its derivative  $\dot{f}(t)$ . In our numerical simulations we start with all particles confined in a narrow stripe, leading us to use  $t_0 = 0$  in Eq. (11). The case  $D = 1$  corresponds to  $N = 3600$  particles with confining potential strength  $k = 3.2 \times 10^{-3} \epsilon / \sigma^2$ . The case  $D = 2$  corresponds to  $N = 4000$  particles, with confining potential strength  $k = 1 \times 10^{-3} \epsilon / \sigma^2$ , in a cell with transverse size  $L_y = 20\sigma$ .

these curves, we performed the Kernel Density Estimation [22] for the position of the particles scaled by the length  $f(t)$  obtained from Eq. (11). The results from simulation are in perfect agreement with the predicted form given by Eq. (9), showing that, in fact, Eq. (11) yields the correct position  $f(t)$  at the edge of the density profile.

Next we proceed to investigate the velocity of particles during the dynamics. To obtain a solution for our non-linear diffusion, Eq. (4), and considering the similarity hypothesis, Eq. (5), from Eq. (9) it is visible that  $g(1) = 0$ , that is,  $f(t)$  is the position where the density profile vanishes. It is reasonable to assume that the average velocities of the particles at a given position and time,  $\bar{v}(x, t)$ , also obey Eq. (5),

$$\bar{v}(x, t) = \dot{f}(t)b(z), \text{ with } \dot{f}(t) = df/dt. \quad (12)$$

The average velocity of the particles at the edge of the density profile is given by  $\bar{v}(f(t), t) = \dot{f}(t)$ . By inserting the similarity hypothesis into the continuity equation, we obtain

$$-\frac{\dot{f}}{f^2} \frac{d}{dz} (gz) = -\frac{\dot{f}}{f^2} \frac{d}{dz} (gb), \quad (13)$$

leading to the condition that  $\bar{v}(x, t) = (\dot{f}/f)x$ , that is, the average velocity is linear with position.

In one dimension there is not more than one particle at each given position  $x$ , therefore if  $\bar{v}(x, t)$  is linear with  $x$ , the velocity of each particle should be linear with  $x$ , leading to the conclusion that they are distributed in the

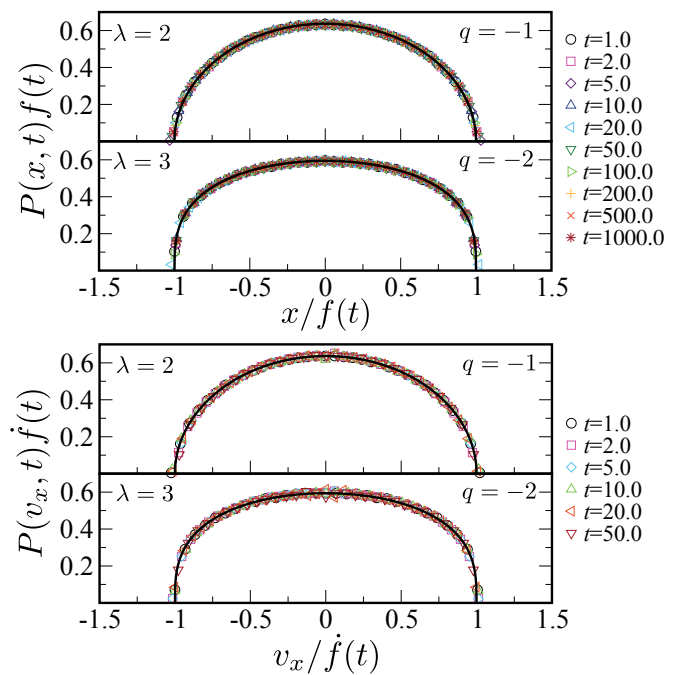


FIG. 3. Distributions of scaled positions and velocities at different moments of the dynamics for the one dimensional case ( $D = 1$ ). These results concern  $N = 3600$  particles interacting through the power law potential,  $V = \epsilon(r/\sigma)^{-\lambda}$ , for  $\lambda = 2$  ( $q = -1$ ) and  $\lambda = 3$  ( $q = -2$ ). The black curves are  $q$ -Gaussians. Here we used the strength of the confining potential  $k = 3.2 \times 10^{-3} \epsilon / \sigma^2$ .

same form, namely, a  $q$ -Gaussian. This prediction is consistent with [23], and confirmed by the results of Fig. 3. In larger dimensionalities there are several particles in the stripe around a given distance  $x$ . In this case  $\bar{v}(x, t)$  may still be linear with  $x$ , but the velocities of each particle may fluctuate around this average.

To test this hypothesis we performed simulations in two dimensions. Figure 4 presents the density profiles and velocity distributions obtained from simulations. As before, positions were scaled by  $f(t)$ , while velocities were scaled by  $\dot{f}(t)$ . As exhibited, the density profiles follow closely the  $q$ -Gaussian form. The velocity distributions also display an invariant shape for all instants. However, this shape deviates slightly from the expected  $q$ -Gaussian form at the largest velocities. Note that to reduce fluctuations in our results we performed averages over 800 sample simulations. To investigate this small difference, we analyze the distribution of the quantity  $\xi_i \equiv (v_x)_i / \dot{f} - x_i / f$  among the particles of all samples, which measures how far  $(v_x)_i$  is from the expected average  $\bar{v}(x_i, t) = (\dot{f}/f)x_i$  for a particle at position  $x_i$  at time  $t$ . Figure 5 shows the distributions  $P(\xi)$  for different values of  $t$ . One can see that  $P(\xi)$  can be described approximately by a Laplacian distribution,

$$P(\xi) \sim \exp(-|\xi|/h), \quad (14)$$

where the parameter  $h$  depends on the particular value

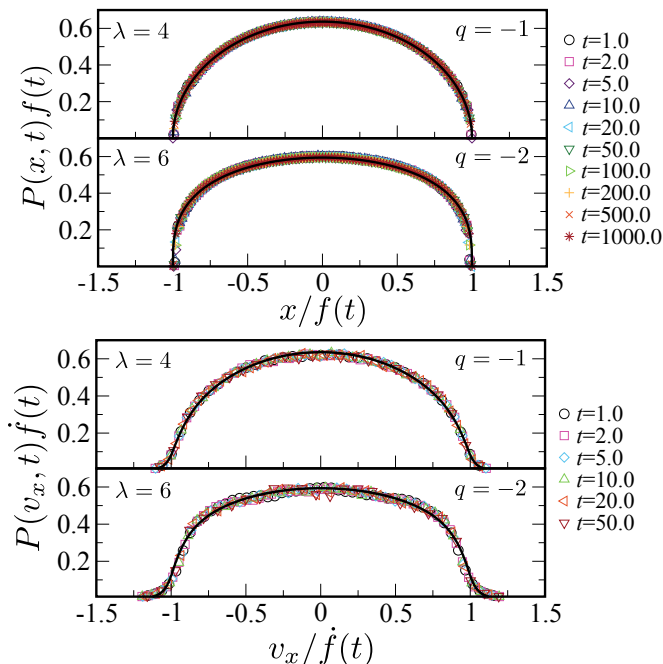


FIG. 4. Distributions of scaled positions and velocities at different moments of the dynamics for the case of two dimensions ( $D = 2$ ). These results concern particles interacting through the power law potential,  $V = \epsilon(r/\sigma)^{-\lambda}$ , for  $\lambda = 4$  ( $q = -1$ ) and  $\lambda = 6$  ( $q = -2$ ). One can compare the density profiles with  $q$ -Gaussians (black curves). In the case of the velocity distributions the black curves show convolutions between  $q$ -Gaussians and Laplacian distributions, as given by Eq. (15), with the parameter  $h$  given by 0.045 and 0.051 for  $\lambda = 4$  and 6, respectively. In these simulations we used  $N = 4000$  particles in a cell of transverse size  $L_y = 20\sigma$  with periodic boundary conditions. In the longitudinal direction ( $x$  axis) we imposed a confining force  $-kx$  with  $k = 1 \times 10^{-3}\epsilon/\sigma^2$ .

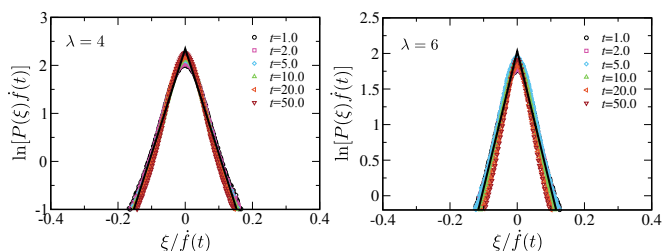


FIG. 5. Distributions of the displacement of the average velocity,  $\xi_i = (v_x)_i/f - x_i/f$  for some values of times  $t$  considering  $\lambda = 4$  and  $\lambda = 6$  for  $D = 2$ . The black curves represent Laplacian distributions,  $P(\xi) \sim \exp(-|\xi|/h)$ , where  $h$  is an adjustment parameter, given by 0.045 and 0.051 for  $\lambda = 4$  and 6, respectively.

of  $\lambda$ . Most likely, these small deviations in the expected value of the velocity are due to the rearrangement of the local spatial structure as the density changes. As we know from the results of Fig. 5, the distribu-

tion of positions can be well described as a  $q$ -Gaussian,  $P(x/f) = G_q(x/[(q-1)f])$ . Since  $f(t)$  and  $\dot{f}(t)$  depend only on time, and  $(v_x)_i/\dot{f} = x_i/f + \xi_i$ , then the  $v_x$ -distribution can be found by the convolution [24] between a  $q$ -Gaussian and a Laplacian distribution,

$$P\left(\frac{v_x}{\dot{f}}\right) = \frac{1}{2h} \int_{-\infty}^{\infty} d\xi G_q\left(\frac{v_x/\dot{f} - \xi}{q-1}\right) e^{-\frac{|\xi|}{h}}. \quad (15)$$

The black curves shown in the Fig. 4 have been obtained from Eq. (15), where the values of  $h$  were obtained from the best fits to the molecular simulation data of the Laplace distribution, Eq. (14), as shown in Fig. 5.

#### IV. DISCUSSION

We have studied a system of particles interacting through power-law repulsive potentials, and under overdamped motion. In a previous work, through a coarse-graining approximation, this model was related to a nonlinear diffusion equation, whose stationary-state solutions have been shown to be compatible with results obtained from molecular-dynamics simulation [13]. Here, we investigate the whole time evolution. Using a similarity hypothesis, we showed that our nonlinear diffusion equation predicts that, for all times, the probability distribution for the positions,  $P(x, t)$ , is a  $q$ -Gaussian with the value of  $q$  depending on both the repulsive potential as well as on dimensionality of the system,  $q = 1 - \lambda/D$ . We present quite satisfactory results from molecular dynamics simulations to give support to the analytic predictions. Moreover, we have also presented results for the  $x$ -component velocity probability distribution,  $P(v_x, t)$ , showing that it is given by a  $q$ -Gaussian distribution that, in larger dimensionalities, will be perturbed by a small extra noise well approximated by a Laplacian distribution. We conjecture that these perturbations are due to the rearrangement of the local spatial structure as the density changes. To summarize, we have presented broad evidence that a system of overdamped repulsive particles interacting through a short-range power-law potential constitutes an important physical application for nonextensive statistical mechanics. Both stationary states and time-dependent properties of the systems are fully compatible with the theory.

#### ACKNOWLEDGMENTS

The authors thank the Brazilian agencies CNPq, CAPES, FUNCAP, and the National Institute of Science and Technology for Complex Systems (INCT-SC) in Brazil for financial support.

- 
- [1] P. G. de Gennes, *Superconductivity of Metals and Alloys* (Benjamin, New York, 1966).
- [2] H. J. Jensen, A. Brass, and A. J. Berlinsky, Phys. Rev. Lett. **60**, 1676 (1988); O. Pla and F. Nori, Phys. Rev. Lett. **67**, 919 (1991); R. A. Richardson, O. Pla, and F. Nori, Phys. Rev. Lett. **72**, 1268 (1994); W. Barford, W. H. Beere, and M. Steer, J. Phys. Condens. Matter **5**, L333 (1993).
- [3] C. Reichhardt, C. J. Olson, J. Groth, S. Field, and F. Nori, Phys. Rev. B **52**, 10441 (1995); Phys. Rev. B **53**, R8898 (1996); C. Reichhardt, J. Groth, C. J. Olson, S. B. Field, and F. Nori, Phys. Rev. B **54**, 16108 (1996); Phys. Rev. B **56**, 14196 (1997).
- [4] O. Pla, N. Wilkin, and H. Jensen, Europhys. Lett. **33**, 297 (1996); C. J. Olson, C. Reichhardt, and F. Nori, Phys. Rev. B **56**, 6175 (1997); Phys. Rev. Lett. **80**, 2197 (1998).
- [5] S. Zapperi, A. A. Moreira, and J. S. Andrade, Phys. Rev. Lett. **86**, 3622 (2001).
- [6] J. S. Andrade, G. F. T. da Silva, A. A. Moreira, F. D. Nobre, and E. M. F. Curado, Phys. Rev. Lett. **105**, 260601 (2010).
- [7] P. Barrozo, A. A. Moreira, J. A. Aguiar, and J. S. Andrade, Phys. Rev. B **80**, 104513 (2009); A. A. Moreira, J. S. Andrade, J. Mendes Filho, and S. Zapperi, Phys. Rev. B **66**, 174507 (2002).
- [8] P. K. Shukla, *Introduction to Dusty Plasma Physics* (CRC Press, Abingdon, 2002).
- [9] H. Totsuji, Physics of Plasmas **8** (2001).
- [10] D. Lucena, D. V. Tkachenko, K. Nelissen, V. R. Misko, W. P. Ferreira, G. A. Farias, and F. M. Peeters, Phys. Rev. E **85**, 031147 (2012); J. E. Galván-Moya, D. Lucena, W. P. Ferreira, and F. M. Peeters, Phys. Rev. E **89**, 032309 (2014).
- [11] W. P. Ferreira, F. F. Munarin, G. A. Farias, and F. M. Peeters, J. Phys. Condens. Matter **18**, 9385 (2006).
- [12] M. Kong, B. Partoens, and F. M. Peeters, New Journal of Physics **5**, 23 (2003).
- [13] C. M. Vieira, H. A. Carmona, J. S. Andrade, and A. A. Moreira, Phys. Rev. E **93**, 060103 (2016).
- [14] A. M. Souza, R. F. Andrade, F. D. Nobre, and E. M. Curado, Physica A **491**, 153 (2018).
- [15] S. Umarov, C. Tsallis, and S. Steinberg, Milan J. Math **76**, 307 (2008); C. Tsallis, Journal of Statistical Physics **52**, 479 (1988); C. Tsallis, R. Mendes, and A. Plastino, Physica A **261**, 534 (1998).
- [16] A. B. Adib, A. A. Moreira, J. S. Andrade, and M. P. Almeida, Physica A **322**, 276 (2003).
- [17] M. L. Lyra, U. M. S. Costa, R. N. C. Filho, and J. S. Andrade, Europhys. Lett. **62**, 131 (2003).
- [18] J. S. Andrade, M. P. Almeida, A. A. Moreira, and G. A. Farias, Phys. Rev. E **65**, 036121 (2002).
- [19] M. S. Ribeiro, F. D. Nobre, and E. M. F. Curado, Phys. Rev. E **85**, 021146 (2012).
- [20] M. Ribeiro, F. Nobre, and E. Curado, Eur. Phys. J. B **85**, 399 (2012).
- [21] V. Bryksin and S. Dorogovtsev, Zh. Eksp. Teor. Fiz **104**, 3735 (1993).
- [22] E. Parzen, The Annals of Mathematical Statistics **33**, 1065 (1962).
- [23] A. R. Plastino, E. M. F. Curado, F. D. Nobre, and C. Tsallis, Phys. Rev. E **97**, 022120 (2018).
- [24] R. V. Hogg and A. T. Craig, *Introduction to Mathematical Statistics* (Macmillan Publishing, New York, 1970).